Dynamic Analysis of Earthen Dams by the Method of Finite Elements

by

S.K. Parikh*

Introduction

IN a previous article(1) the finite element method of analysis was presented for determining stress and deformation patterns developed due to the self-weight of an earthen dam. Besides various static loads, there may also be dynamic loads due to natural causes such as earthquake shocks.

Conventionally the effects of such a shock would be determined by following a design procedure which may be termed as pseudo-static analysis. For example in the pseudo-static analysis of the finite element idealization shown in Figure 1, the quake shock would be treated as equivalent static load defined by an appropriate value of the seismic coefficient '*K*' (Figure 2).

In case of the routine design procedures, the pseudo-static analysis would involve the stability checking of the potential sliding mass with the seismic forces imposed upon it as shown in Figure 3. This kind of design procedure has, however, been shown to be too inadequate to indicate the

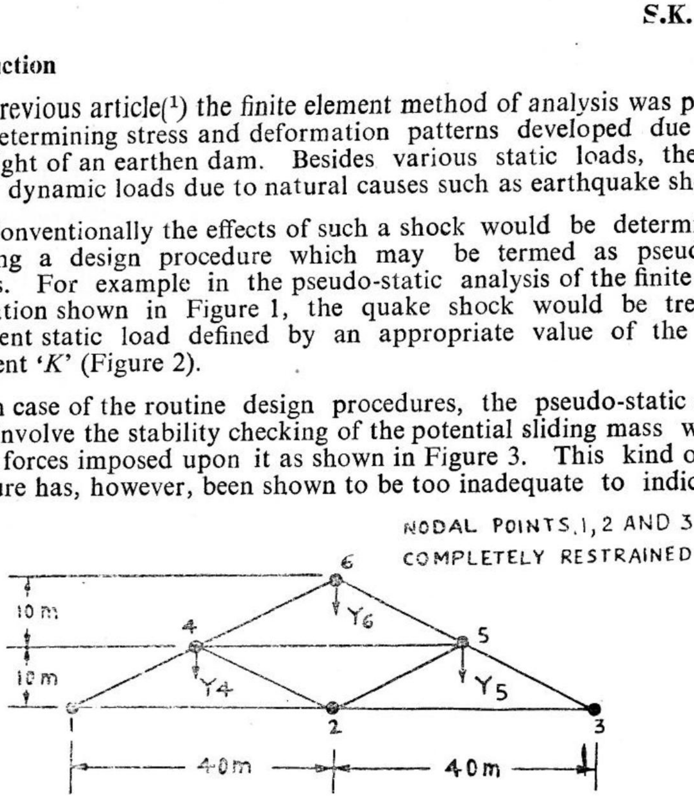

FIGURE 1.

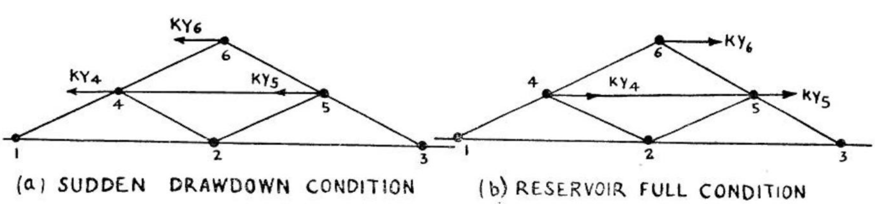

FIGURE 2.

* Lecturer in Civil Engineering, College of Engineering, Poona-5.

This paper was received on 22 July 1970. It is open for discussion up to September 1971.

true response of the earthen dams subjected to seismic shocks(2). This means pseudo-static finite element method of analysis may also prove to be incapable of predicting the true seismic response. Thus a method that takes into account the dynamic nature of the seismic forces may be necessary towards rational aseismic design of earthen dams.

The finite element dynamic analysis may be carried out by following the standard procedure employed in the dynamic analysis of a lumped mass structural system. In the present article the method is discussed at length with reference to the development of the dynamic displacements of the finite element idealization shown in Figure 4 (*a*). In the analysis it will be assumed that the base of the system is shaken by an earthquake shock of the type shown in Figure 4 (*b*). In reality the quake shock would never be so uniform. On the contrary it would be quite random. However the method that would be demonstrated does not take advantage of the uniformity of the selected shock, hence it is justified to use the same for the sake of simplicity.

While discussing the dynamic analysis the damping offered by the dam is ignored. Actually the damping is one of the most important factors governing the true dynamic response ; but its consideration in the present article is considered to be beyond the scope due to following reasons :—

(*a*) The nature of damping in an earthen mass is a very complex phenomenon. To include it in the analysis some kind of oversimplification would be necessary. To appreciate the limitations of the proposed oversimplification the factors which govern the damping should be discussed at length beforehand. This in itself would justify a full length independent article.

(*b*) Once the oversimplification is accepted the inclusion of damping involves only additional computational efforts. As the purpose

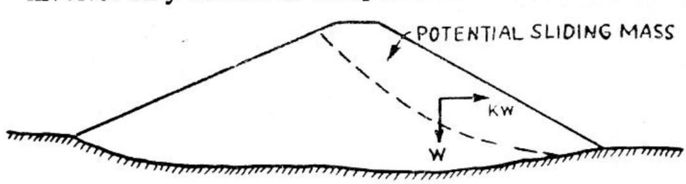

FIGURE 3.

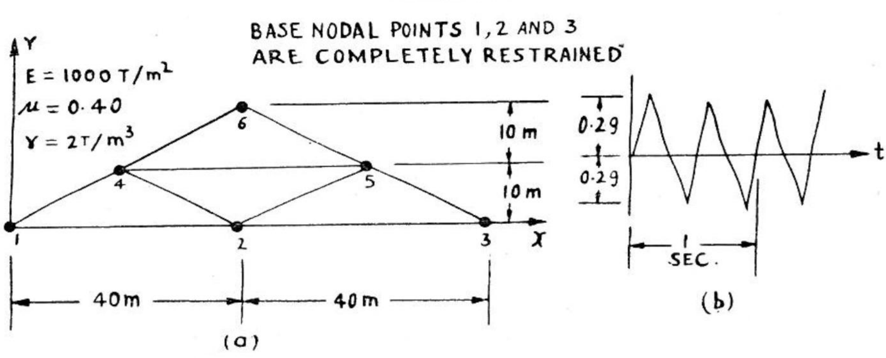

FIGURE 4.

of the present article is to discuss the concepts behind the dynamic analysis, the ommission of this extra computation would simplify the presentation.

Natural Vibration Character

The idealised system shown in Figure 4 (*a*) may be considered to be a lumped mass system with one-third mass of each element concentrated at their nodal points, so that the masses are interconnected through massless triangular elements with specific stiffness character $[K]$ (Figure 5).

With the base nodal points 1, 2 and 3 completely restrained, the masses m_1, m_2 and m_3 cannot vibrate under the influence of any dynamic load. *The masses m_4, m_5 a m_6 are, however, free to vibrate both in 'x'* as well as the '*y*' direction. The system thus has six degree of freedom for vibration.

Just as a pendulum would indefinitely go on swinging, once set into motion, in absence of damping, the idealised system will also vibrate indefinitely in its own plane once set into motion. As the system possesses six degree of freedom for vibration, it can vibrate indefinitely with six different natural frequencies having correspondingly six different modes of vibration(3). These frequencies and the modes of vibration are the natural inherent character of the system. Their knowledge helps in carrying out the dynamic analysis.

Eigen Value Problem

Applying the principles of dynamics to masses m_4, m_5 and m_6, it follows that the natural vibration character of the system will be represented by Equation (1) in matrix form

$$[m]\,[\ddot{r}] + [K]\,[r] = 0 \qquad \ldots(1)$$

Where various matrices in the equation have the following meaning:—

(*a*) $[r]$—Nodal displacement matrix :

The nodal displacement matrix is given by Equation (2).

$$[r] = \begin{bmatrix} r_{x_4} \\ r_{y_4} \\ r_{x_5} \\ r_{y_5} \\ r_{x_6} \\ r_{y_6} \end{bmatrix} \qquad \ldots(2)$$

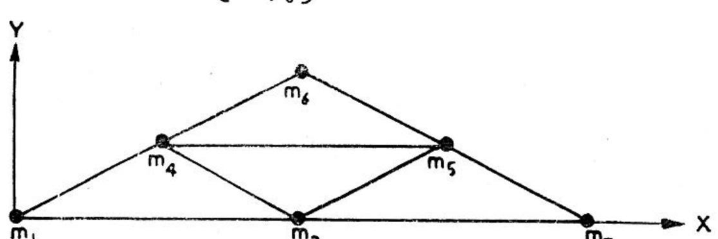

FIGURE 5.

(*b*) [$\ddot{\mathbf{r}}$]—Nodal acceleration matrix :

The nodal acceleration matrix is given by Equation (3).

$$[\ddot{\mathbf{r}}] = \frac{\partial^2}{\partial t^2}\,[r] = \begin{bmatrix} \ddot{\mathbf{r}}_{x_4} \\ \ddot{\mathbf{r}}_{y_4} \\ \ddot{\mathbf{r}}_{x_5} \\ \ddot{\mathbf{r}}_{y_5} \\ \ddot{\mathbf{r}}_{x_6} \\ \ddot{\mathbf{r}}_{y_6} \end{bmatrix} \qquad \ldots(3)$$

(*c*) [m]—Nodal mass matrix :

The mass of various triangular elements is assumed to be lumped at their nodal points. Each element has a mass of

$$\frac{2\times\frac{1}{2}\times 40\times 10}{9{\cdot}81} = 40{\cdot}78 \text{ T.}$$

One-third of this mass is lumped at each nodes so :

$$m_1 = m_3 = m_6 = \tfrac{1}{3}\times 40{\cdot}78 = 13{\cdot}59 \text{ T.}$$
$$m_2 = m_4 = m_5 = 3\times\tfrac{1}{3}\times 40{\cdot}78 = 13{\cdot}59\times 3 \text{ T.}$$

As the base nodal points 1, 2 and 3 are completely restrained, only m_4, m_5 and m_6 are involved in vibration. So the nodal mass matrix is the diagonal matrix as shown in Equation (4).

$$[m] = 13{\cdot}59\times \begin{bmatrix} 3 & & & & & \\ & 3 & & & & \\ & & 3 & & & \\ & & & 3 & & \\ & & & & 1 & \\ & & & & & 1 \end{bmatrix} \qquad \ldots(4)$$

(*d*) [K]—Stiffness matrix :

The structural stiffness matrix had been derived in an earlier article[1] *and it is as shown in Equation (5).*

$$[K] = 2{\cdot}68\times \begin{bmatrix} 0601 & 0000 & 0-66 & 0000 & -133 & -267 \\ 0000 & 2434 & 0000 & 0766 & -\ 67 & -800 \\ -66 & 0000 & 0601 & 0000 & -133 & 267 \\ 0000 & 766 & 0000 & 2434 & 67 & -800 \\ -133 & -67 & -133 & 67 & 267 & 000 \\ -267 & -800 & 267 & -800 & 000 & 1600 \end{bmatrix} \qquad \ldots(5)$$

Let $r = a \sin wt$ ...(6)

where,

a = half amplitude of vibration and

w = the circular frequency of vibration.

Then :

$$\ddot{r} = -a\,w^2 \sin wt = -w^2 . r \qquad ...(7)$$

Substituting Equation (7) in Equation (1) and putting $w^2 = B$, Equation (8) is obtained.

$$B\,[m]\,[r] = [K]\,[r] \qquad ...(8)$$

Equation (8) represents an Eigen value or characteristics value problem for the system. Its solution would establish the normal vibration character of the idealised system.

Solution of Eigen Value Problem

Substituting the values of $[m]$ and $[K]$ from Equations (4) and (5) into Equation (8) and rearranging the terms, Equation (9) is obtained

$$[L]\,[r] = 0 \qquad ...(9)$$

Where $[L]$ is given in Table I.

TABLE I

$$[L] = \begin{bmatrix} 39{\cdot}5 - B & 0 & -4{\cdot}34 & 0 & -8{\cdot}74 & -17{\cdot}6 \\ -0 & 160 - B & 0 & 50{\cdot}3 & -4{\cdot}40 & -52{\cdot}6 \\ -4{\cdot}34 & 0 & 39{\cdot}5 - B & 0 & -8{\cdot}74 & 17{\cdot}6 \\ 0 & 50{\cdot}3 & 0 & 160 - B & 4{\cdot}40 & -52{\cdot}6 \\ -26{\cdot}2 & -13{\cdot}2 & -26{\cdot}2 & 13{\cdot}2 & 52{\cdot}60 - B & 0 \\ -52.6 & -157{\cdot}8 & 52{\cdot}6 & -157{\cdot}8 & 0 & 315{\cdot}6 - B \end{bmatrix}$$

As may be noted, Equation (9) is representing a set of six homogeneous equations. For its non-trivial solution the characteristic determinant $| L |$ should be equal to zero. The nature of matrix $[L]$ in Table I clearly indicates that the above condition leads to a polynomial in 'B' of six degree as shown by Equation (10).

$$(B-B_1)\,(B-B_2)\,(B-B_3)\,(B-B_4)\,(B-B_5)\,(B-B_6) = 0 \qquad ...(10)$$

Thus there are six values of 'B' such as $B_1, B_2 ... B_6$, satisfying the condition for non-trivial solution. These values of 'B' give six values of frequencies such as $w_1, w_2 ...... w_6$ *etc.*

Substituting each of the values of 'B' in Equation (9), six sets each having six homogeneous equations would be obtained as shown in Equation (11).

$$[L_1]\,[r] = [L_2]\,[r] = ...[L_6]\,[r] = 0 \qquad ...(11)$$

The solution of any of the sets say $[L_n]\,[r] = 0$ gives rise to the relative nodal displacements. Keeping one of the nodal displacements to be unity the values of other nodal displacements are obtained. Such set of six nodal displacements constitutes the nth mode shape character and it may be denoted by $[\phi_n]$. This mode shape will have frequency of vibration of 'w_n'.

The complete solution of Equation (11) would thus give six mode shapes $[\phi_1]$, $[\phi_2]$......$[\phi_6]$ corresponding to six frequencies of vibration $w_1, w_2 ...... w_6$.

Numerical Solution for Mode Shapes and Frequencies

The method of matrix iteration coupled with the condition of the mutual orthogonality of the mode shapes would be employed for the numerical solution of the eigen value problem. The method presented here in essence follows the procedure adopted by Hurty and Rubunstein[3].

As the stiffness character has been employed in the derivation of the eigen value problem first the mode having highest value of 'w' will get established, *i.e.*, in the present case the 6th mode would get established first.

(a) SIXTH MODE

Equation (9) is rearranged in a form suitable for matrix iteration process as shown in Equation (12). The iteration is demonstrated in Table II. It is assumed that 7th step gives sufficiently accurate result. The 6th mode character is thus as shown in Equation (13).

$$B\,[r] = \begin{bmatrix} 39{\cdot}5 & 0 & -4{\cdot}34 & 0 & -8{\cdot}74 & -17{\cdot}6 \\ 0 & 160 & 0 & 50{\cdot}3 & -4{\cdot}40 & -52{\cdot}6 \\ -4{\cdot}34 & 0 & 39{\cdot}5 & 0 & -8{\cdot}74 & 17{\cdot}6 \\ 0 & 50{\cdot}3 & 0 & 160 & 4{\cdot}40 & -52{\cdot}6 \\ -26{\cdot}2 & -13{\cdot}2 & -26{\cdot}2 & 13{\cdot}2 & 52{\cdot}60 & 0 \\ -52{\cdot}6 & -157{\cdot}8 & 52{\cdot}6 & -157{\cdot}8 & 0 & 315.6 \end{bmatrix} [r] \quad ...(12)$$

$$B_6 = 405{\cdot}6$$

$$w_6 = 20{\cdot}14 \text{ rad/sec.}$$

$$[\phi_6] = \begin{bmatrix} -0{\cdot}04867 \\ -0{\cdot}26890 \\ 0{\cdot}04867 \\ -0{\cdot}26890 \\ 0 \\ 1{\cdot}00000 \end{bmatrix} \quad ...(13)$$

TABLE II

Step 1

$$B \times \begin{bmatrix} 0 \\ 0 \\ 0 \\ 0 \\ 0 \\ 1 \end{bmatrix} = \begin{bmatrix} -17{\cdot}6 \\ -52{\cdot}6 \\ 17{\cdot}6 \\ -52{\cdot}6 \\ 0 \\ 315{\cdot}6 \end{bmatrix} = 315{\cdot}6 \times \begin{bmatrix} -0{\cdot}05577 \\ -0{\cdot}1666 \\ 0{\cdot}05577 \\ -0{\cdot}1666 \\ 0 \\ 1 \end{bmatrix}$$

Step 2

$$B \times \begin{bmatrix} -0\ 05577 \\ -0{\cdot}1666 \\ 0{\cdot}05577 \\ -0{\cdot}1666 \\ 0 \\ 1 \end{bmatrix} = \begin{bmatrix} -20{\cdot}05 \\ -87{\cdot}63 \\ 20{\cdot}05 \\ -87{\cdot}63 \\ 0 \\ 374 \end{bmatrix} = 374 \times \begin{bmatrix} -0{\cdot}0536 \\ -0{\cdot}2343 \\ 0{\cdot}0536 \\ -0{\cdot}2343 \\ 0 \\ 1 \end{bmatrix}$$

Step 3

$$B \times \begin{bmatrix} -0{\cdot}0536 \\ -0{\cdot}2343 \\ 0{\cdot}0536 \\ -0{\cdot}2343 \\ 0 \\ 1 \end{bmatrix} = \begin{bmatrix} -19{\cdot}95 \\ -101\ 90 \\ 19{\cdot}95 \\ -101{\cdot}90 \\ 0 \\ 395{\cdot}20 \end{bmatrix} = 395{\cdot}2 \times \begin{bmatrix} -0{\cdot}05049 \\ -0{\cdot}2577 \\ 0{\cdot}05049 \\ -0{\cdot}2577 \\ 0 \\ 1 \end{bmatrix}$$

Step 4

$$B \times \begin{bmatrix} -0{\cdot}05049 \\ 0{\cdot}2577 \\ -0{\cdot}05049 \\ -0{\cdot}2577 \\ 0 \\ 1 \end{bmatrix} = \begin{bmatrix} -19\ 81 \\ -106{\cdot}80 \\ 19{\cdot}81 \\ -106{\cdot}80 \\ 0 \\ 402{\cdot}3 \end{bmatrix} = 402{\cdot}3 \times \begin{bmatrix} -0{\cdot}04925 \\ -0{\cdot}2656 \\ 0{\cdot}04925 \\ --0{\cdot}2656 \\ 0 \\ 1 \end{bmatrix}$$

TABLE II (*Contd.*)

Step 5

$$B \times \begin{bmatrix} -0{\cdot}04925 \\ -0{\cdot}2656 \\ 0{\cdot}04925 \\ -0{\cdot}2656 \\ 0 \\ 1 \end{bmatrix} = \begin{bmatrix} -19{\cdot}76 \\ -108{\cdot}40 \\ 19{\cdot}76 \\ -108{\cdot}40 \\ 0 \\ 404{\cdot}60 \end{bmatrix} = 404{\cdot}6 \times \begin{bmatrix} -0{\cdot}04884 \\ -0{\cdot}2680 \\ 0{\cdot}04884 \\ -0{\cdot}2680 \\ 0 \\ 1 \end{bmatrix}$$

Step 6

$$B \times \begin{bmatrix} -0{\cdot}04884 \\ -0{\cdot}2680 \\ 0{\cdot}04884 \\ -0{\cdot}2680 \\ 0 \\ 1 \end{bmatrix} = \begin{bmatrix} -19{\cdot}74 \\ -109{\cdot}00 \\ 19{\cdot}74 \\ -109{\cdot}00 \\ 0 \\ 405{\cdot}30 \end{bmatrix} = 405{\cdot}3 \times \begin{bmatrix} -0{\cdot}04871 \\ -0{\cdot}2689 \\ 0{\cdot}04871 \\ -0{\cdot}2689 \\ 0 \\ 1 \end{bmatrix}$$

Step 7

$$B \times \begin{bmatrix} -0{\cdot}04871 \\ -0{\cdot}2689 \\ 0{\cdot}04871 \\ -0{\cdot}2689 \\ 0 \\ 1 \end{bmatrix} = \begin{bmatrix} -19{\cdot}74 \\ -109{\cdot}10 \\ 19{\cdot}74 \\ -109{\cdot}10 \\ 0 \\ 405{\cdot}60 \end{bmatrix} = 405{\cdot}6 \times \begin{bmatrix} -0{\cdot}04867 \\ 0{\cdot}2689 \\ 0{\cdot}04867 \\ -0{\cdot}2689 \\ 0 \\ 1 \end{bmatrix}$$

(b) ORTHOGONALITY OF MODE SHAPES

Imagine a six-dimensional space with six mutually perpendicular axes in such a manner that the six nodal displacements of various mode shapes are represented one on each axis. Due to this the mode shape will be a mode vector in that space. The orthogonality of mode shapes mean that the corresponding modal vectors are mutually orthogonal. The proof is as follows :

Let suffix 'p' and 'q' denote the characteristics of pth and qth mode of vibration According to Equation (8), the nodal forces during the extreme positions of the amplitude of the nodal masses are given by Equation (14)

$$\left.\begin{aligned} & w_p^2\,[m]\,[\phi_p] \\ & w_q^2\,[m]\,[\phi_q] \end{aligned}\right\} \qquad \ldots(14)$$

If the forces in the pth mode are given the virtual displacement of the qth mode then the virtual work is same as would be obtained by giving the virtual displacement of the pth mode to the nodal forces in the qth mode[4].

Hence :

$$w_p^2 \; [\phi_q]^T [m] \, [\phi_p] = w_q^2 \; [\phi_p]^T [m] \, [\phi_q] \qquad ...(15)$$

By using the relationship in Equation (8) it can be proved that for the condition $w_p \neq w_q$, Equation (15) is valid only if :

$$\left. \begin{array}{l} [\phi_q]^T [m] \, [\phi_p] = 0 \\ [\phi_p]^T [m] \, [\phi_q] = 0 \end{array} \right\} \qquad ...(16)$$

Substitution of Equation (16) in Equation (15) proves that virtual works are zero. Hence the mode shapes are orthogonal in the sense described.

(c) USE OF THE CONDITION OF ORTHOGONALITY

Applying the condition of orthogonality expressed by Equation (16) to 5th and 6th mode :

$$[\phi_6]^T [m] \, [\phi_5] = 0 \qquad ...(17)$$

Substituting $[\phi_6]$ and $[m]$ from Equations (13) and (4) into Equation (17), the displacements in the 5th mode would satisfy Equation (18).

$$r_{y_6} = 0{\cdot}146 \, r_{x_4} + 0{\cdot}8067 \, r_{y_4} - 0{\cdot}146 \, r_{x_5} + 0{\cdot}8067 \, r_{y_5}. \qquad ...(18)$$

Substitution of Equation (18) in Equation (12) will give the matrix equation valid for the 5th mode shape (Table III). Its comparison with Equation (12) indicates that one of the columns has been swept away. This makes iteration process for the 5th mode relatively more easy. In fact while establishing further lower mode shapes at each stage the condition of orthogonality would sweep out one additional column at each successive modes (as may be noted in Table III), making computational work more and more easier.

TABLE III

5th mode

$$B\,[r] = \begin{bmatrix} 36{\cdot}9 & -14{\cdot}2 & -1{\cdot}77 & -14{\cdot}2 & -8{\cdot}74 & 0 \\ -7{\cdot}68 & 117{\cdot}6 & 7{\cdot}68 & 7{\cdot}87 & -4{\cdot}40 & 0 \\ -1{\cdot}77 & 14{\cdot}2 & 36{\cdot}9 & 14{\cdot}2 & -8{\cdot}74 & 0 \\ -7{\cdot}68 & 7{\cdot}87 & 7{\cdot}68 & 117{\cdot}6 & 4{\cdot}40 & 0 \\ -26{\cdot}2 & -13{\cdot}2 & -26{\cdot}20 & 13{\cdot}2 & 52{\cdot}60 & 0 \\ -6{\cdot}60 & 96{\cdot}8 & 6{\cdot}60 & 96{\cdot}8 & 0 & 0 \end{bmatrix} [r]$$

TABLE III (*Contd.*)

4th mode

Substituting $[\phi_6]^T[m]\,[\phi_4] = [\phi_5]^T[m]\,[\phi_4] = 0$

$$r_{y_5} = 0{\cdot}168\, r_{x_4} - r_{y_4} - 0{\cdot}168\, r_{x_5}$$

$$B\,[r] = \begin{bmatrix} 34{\cdot}5 & 0 & 0{\cdot}60 & 0 & -8{\cdot}74 & 0 \\ -6{\cdot}36 & 109{\cdot}7 & 6{\cdot}36 & 0 & -4{\cdot}40 & 0 \\ 0{\cdot}60 & 0 & 34{\cdot}5 & 0 & -8{\cdot}74 & 0 \\ 12{\cdot}1 & -109{\cdot}7 & -12{\cdot}1 & 0 & 4{\cdot}40 & 0 \\ -24 & -26{\cdot}4 & -28{\cdot}4 & 0 & 52{\cdot}60 & 0 \\ 9{\cdot}70 & 0 & -9{\cdot}70 & 0 & 0 & 0 \end{bmatrix} [r]$$

3rd mode

$$[\phi_6]^T\,[m]\,[\phi_3] = \ldots\ldots[\phi_4]^{\mathrm{T}}\,[m]\,[\phi_3] = 0$$

$$r_{y_4} = -0{\cdot}0009\, r_{x_4} - 0{\cdot}1689\, r_{x_5} + 0{\cdot}248\, r_{x_6}\,.$$

$$B\,[r] = \begin{bmatrix} 34{\cdot}5 & 0 & 0{\cdot}6 & 0 & -8{\cdot}74 & 0 \\ -6{\cdot}5 & 0 & -12{\cdot}2 & 0 & 22{\cdot}80 & 0 \\ 0{\cdot}6 & 0 & 34{\cdot}5 & 0 & -8{\cdot}74 & 0 \\ 12{\cdot}2 & 0 & 6{\cdot}5 & 0 & -22{\cdot}80 & 0 \\ -24 & 0 & -24 & 0 & 46{\cdot}10 & 0 \\ 9{\cdot}7 & 0 & -9{\cdot}70 & 0 & 0 & 0 \end{bmatrix} [r]$$

2nd mode

$$[\phi_6]^T\,[m]\,[\phi_2] = \ldots\ldots[\phi_3]^T\,[m]\,[\phi_2] = 0$$

$$r_{x_6} = 0{\cdot}662\, r_{x_4} + 0{\cdot}622\, r_{x_5}\,.$$

$$B\,[r] = \begin{bmatrix} 28{\cdot}7 & 0 & -5{\cdot}2 & 0 & 0 & 0 \\ 8{\cdot}6 & 0 & 2{\cdot}9 & 0 & 0 & 0 \\ -5{\cdot}2 & 0 & 28{\cdot}7 & 0 & 0 & 0 \\ -2{\cdot}9 & 0 & -8{\cdot}6 & 0 & 0 & 0 \\ 6{\cdot}5 & 0 & 6{\cdot}5 & 0 & 0 & 0 \\ 9{\cdot}7 & 0 & -9{\cdot}7 & 0 & 0 & 0 \end{bmatrix} [r]$$

1st mode

$$[\phi_6]^T [m] [\phi_1] \ldots\ldots [\phi_2]^T [m] [\phi_1] = 0$$

$$r_{x_4} = r_{x_5}.$$

$$B[r] = \begin{bmatrix} 23{\cdot}5 & 0 & 0 & 0 & 0 & 0 \\ 11{\cdot}5 & 0 & 0 & 0 & 0 & 0 \\ 23{\cdot}5 & 0 & 0 & 0 & 0 & 0 \\ -11{\cdot}5 & 0 & 0 & 0 & 0 & 0 \\ 13{\cdot}0 & 0 & 0 & 0 & 0 & 0 \\ 0 & 0 & 0 & 0 & 0 & 0 \end{bmatrix} [r]$$

(d) COMPARISON OF MODE CHARACTERISTICS

Table III indicates the complete solution of the eigen value problem. The solution has been obtained by solving the matrix equations presented in Table III. The mode shapes are shown graphically in Figure 6. It may be seen that both symmetrical as well as anti-symmetrical modes of vibrations are excited. For example 1st, 3rd and 4th modes are anti-symmetrical, whereas 2nd, 5th and 6th modes are symmetrical.

TABLE IV

Mode	1st mode	2nd mode	3rd mode	4th mode	5th mode	6th mode
w	4·848	5 822	7·861	10·57	11·41	20·14
r_{x_4}	1·0000	1·0000	—0·3270	0·0566	−0 2043	−0·04867
r_{y_4}	0·4894	0·1682	0·4678	1·0000	0·6590	—0·26890
r_{x_5}	1·0000	—1·0000	—0·3270	0·0566	0·2043	0·04867
r_{y_5}	—0·4894	0·1682	—0·4678	—1·0000	0·6590	—0·26890
r_{x_6}	0·5531	0·0000	1·0000	—0·4590	0·0000	0.00000
r_{y_6}	0·0000	0·5723	0·0000	0 0000	1·0000	1·00000

Note : 'w' are in radians/sec.

Nodal Dynamics

As shown in Figure 4(b), the base of the idealized system is subjected to quake acceleration of $f(t) \times 0{\cdot}2\ g$, where $f(t)$ is a function of time describing the time variation of the intensity of the shock. It is stated that(5) effective force induced in a structure by an earthquake acceleration of $f(t) \times 0{\cdot}2\ g$ applied at the base is equal to the lumped mass at each nodal

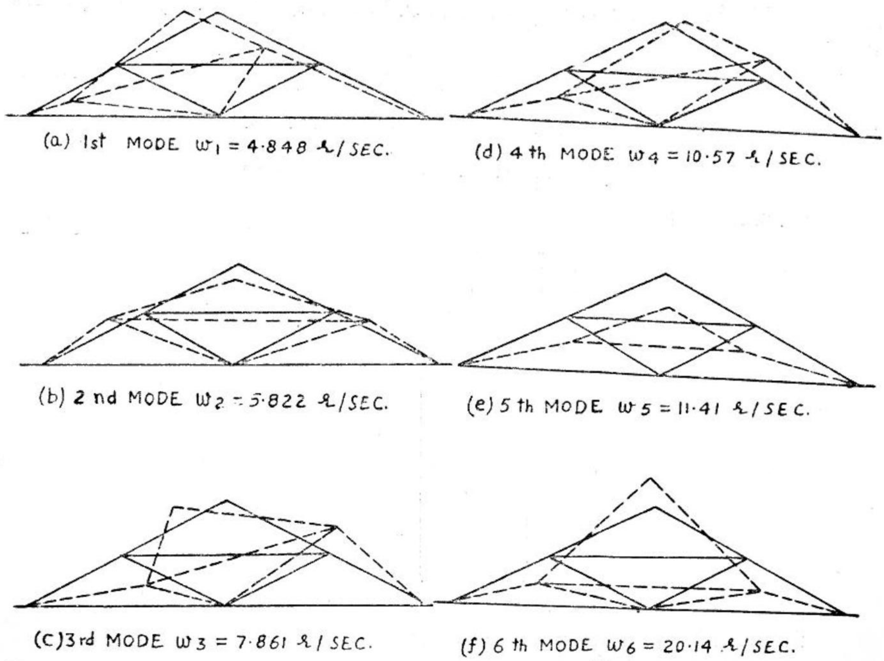

(a) 1st MODE $\omega_1 = 4{\cdot}848$ R/SEC.

(d) 4 th MODE $\omega_4 = 10{\cdot}57$ R/SEC.

(b) 2 nd MODE $\omega_2 = 5{\cdot}822$ R/SEC.

(e) 5 th MODE $\omega_5 = 11{\cdot}41$ R/SEC.

(c) 3rd MODE $\omega_3 = 7{\cdot}861$ R/SEC.

(f) 6 th MODE $\omega_6 = 20{\cdot}14$ R/SEC.

FIGURE 6.

point multiplied by the earthquake acceleration and it acts in the direction opposite to it.

The nodal dynamics would thus be described by Equation (19).

$$[m]\,[\ddot{r}]+[K]\,[r]=-f(t).\,[m]\,[a] \qquad ..(19)$$

Where $-[a]$ is the base acceleration matrix given by Equation (20).

$$[a]=\begin{bmatrix} 0.2\,g \\ 0 \\ 0{\cdot}2\,g \\ 0 \\ 0{\cdot}2\,g \\ 0 \end{bmatrix} \qquad ..(20)$$

Equation (19) represents a set of six differential equations, whose simultaneous or coupled solution would be extremely difficult. These equations can, however, be decoupled by utilising the natural vibration character shown in Table IV. The derivation is given below :

Actual mode of vibration excited in the system by the quake shock may be viewed as weighted sum of the fundamental modes of vibration shown in Table IV. So the dynamic nodal displacements may be represented by Equation (21)

$$[r]=R_1[\phi_1]+R_2[\phi_2]+\ldots R_6[\phi_6] \qquad \ldots(21)$$

Where R_1, $R_2 \ldots R_6$ *etc.*, are mode superposition factors.

Equation (21) may be rewritten as Equation (22).

Where

$$[r]=[\phi]\,[R] \qquad \ldots(22)$$

$$[\phi]=[\phi_1,\ \phi_2\ldots\phi_6]$$

$$[R]=\begin{bmatrix} R_1 \\ R_2 \\ \ldots \\ \ldots \\ \ldots \\ R_6 \end{bmatrix}$$

Substituting Equation (22) in Equation (19) :

$$[m]\,[\phi]\,[\ddot{R}]+[K]\,[\phi]\,[R]=-f(t).[m]\,[a] \qquad \ldots(23)$$

Premultiplying Equation (23) by $[\phi]^T$

$$[\phi]^T[m]\,[\phi][\ddot{R}]+[\phi]^T[K]\,[\phi]\,[R]=-f(t)\cdot[\phi]^T[m]\,[a] \qquad \ldots(24)$$

Various matrices in Equation (24) can be simplified as shown below :

(*i*) $[\phi]^T[m]\,[\phi]$:

Utilising the orthogonality of the mode shapes $[\phi]^T[m]\ [\phi]$ can be proved to be a diagonal matrix shown by Equation (25).

$$\begin{bmatrix} (m_4 r^2_{x_4}+\ldots\ldots m_6 r^2_{y_6})_1 & & & & \\ & \cdot & & & \\ & & \cdot & & \\ & & & \cdot & \\ & & & & \cdot \\ & & & & & (m_4 r^2_{x_4}+\ldots\ldots m_6 r^2_{y_6})_6 \end{bmatrix} \qquad \ldots(25)$$

where suffix 1,......6, *etc.*, applied outside the bracket indicate the mode numbers.

As already pointed out the mode shapes represent only the relative displacements, hence a fresh selection (*i.e.*, one different form those shown in Table IV) of their values may be so made that :

$$(m_4 r^2_{x_4} + \dots m_6 r^2_{y_6})_1 = \dots (m_4 r^2_{x_4} + \dots m_6 r^2_{y_6})_6 = 1 \qquad \dots(26)$$

With the above substitution in Equation (25) the matrix $[\phi]^T [m] [\phi]$ is transformed into a unit diagonal matrix.

(*ii*) $[\phi]^T [K] [\phi]$:

Using Equation (8) and the unit diagonal character of the matrix $[\phi]^T [m] [\phi]$ it can be shown that $[\phi]^T [K] [\phi]$ is also a diagonal matrix shown by Equation (27)

$$[\phi]^T [K][\phi] = \begin{bmatrix} \searrow & & & & & & \\ & w_1^2 & & & & & \\ & & w_2^2 & & & & \\ & & & \cdot & & & \\ & & & & \cdot & & \\ & & & & & \cdot & \\ & & & & & & w_6^2 \\ & & & & & & \nwarrow \end{bmatrix} = [w^2] \qquad \dots(27)$$

(*iii*) $[\phi]$:

$[\phi]$ was represented by $[\phi_1 \, \phi_2 \dots \phi_6]$. Now with the condition laid down in Equation (26) $[\phi]$ is transformed into $[\phi]$ where $[\phi] = [\phi_1 \, \phi_2 \dots \phi_6]$. The numerical character of $[\phi]$ is shown in Table V. The $[\phi]$ is called the normalised mode shapes.

TABLE V

ϕ_1	ϕ_2	ϕ_3	ϕ_4	ϕ_5	ϕ_6
0·0975	0·1064	—0·0516	0·0049	—0·0282	0·0177
0·0477	0·0179	0·0739	0·1083	0·0910	C·0975
0·0975	—0·1064	—0·0516	0·0049	0·0282	—0·0177
—0·0477	0·0179	—0·0739	—0·1083	0·0910	0·0975
0·0539	0·0000	0·1575	—0·3571	0·0000	0·0000
0·0000	0·0609	0·0000	0·0000	0·1380	—0·1209

Substitution of the resultant matrices as described above into Equation (24) transforms the set of coupled equations into a set of decoupled equations as shown below :

$$[\ddot{R}]+[w^2]\,[R]=-f(t)\,.\,[\phi]^T[m][a] \qquad \ldots(28)$$

Pseudo-Static Analysis

As mentioned in the introduction of the article, the pseudo-static analysis of the system can be made by the standard finite element method *with reference to the load conditions shown in Figure 2.* The value of seismic coefficient in that case would be 0·2.

The same analysis can also be done more conveniently in the present case by using Equation (28). For example substitution of $[\ddot{R}]=0$ and $f(t)=\pm 1$ into Equation (28) leads to Equation (29) valid for the pseudo-static condition

$$[w^2]\,[R]=\mp[\phi]^T\,[m][a] \qquad \ldots(29)$$

Denoting R_s to represent the value of 'R' in the pseudo-static condition, $[R_s]$ is given by Equation (30).

$$[R_s]=\mp\frac{[\phi]^T\,[m][a]}{[w^2]} \qquad \ldots(30)$$

Various matrices on the right hand side of Equation (30) have already been established so the values of R_s corresponding to various modes are obtained as shown in Table VI.

It may be noted that due to the convention that the forces and displacements are positive in the negative directions of the axes, the substitution of $f(t)=+1$ gives the reservoir full condition whereas $f(t)=-1$ gives the sudden drawdown condition (Table VI).

TABLE VI

Condition of the reservoir	R_{s_1}	R_{s_2}	R_{s_3}	R_{s_4}	R_{s_5}	R_{s_6}
Full	−0·725	0	0 066	0·078	0	0
Sudden drawdown	0·725	0	−0·066	−0·078	0	0

R_s is also called participation factor. It indicates the weightage with which the normalised mode shapes should be superposed so as to obtain the displacement configuration under the pseudo-static loads. Using Equation (22) and normalised mode character from Table V, the pseudo-static displacements are estimated as shown in Table VII.

TABLE VII

Nodal point	Reservoir full condition		Sudden drawdown condition	
	r_x	r_y	r_x	r_y
1	0	0	0	0
2	0	0	0	0
3	0	0	0	0
4	—0·0737	—0·0212	0·0737	0·0212
5	—0·0737	0·0212	0·0737	—0·0212
6	—0·0566	0·0000	0·0566	0·0000

Note : All the displacements are in metres.

Dynamic Analysis

Let the dynamic value of '*R*' be given by Equation (31).

$$R_n = D_n \times R_{s_n} \qquad \text{...(31)}$$

where,

R_n=Dynamic value of R for the nth mode of vibration and it is function of $f(t)$.

R_{s_n}=Pseudo-static value of R for the nth mode, corresponding to the reservoir full condition. It is a constant as shown in Table VI.

D_n=A proportionality constant called as dynamic load factor and it is also function of $f(t)$.

Substitution of Equation (31) in the nth mode expression of Equation (28), it follows that :

$$\ddot{D}_n \times R_{s_n} + w_n^2 \times D_n \times R = -f(t) \, . \, [\phi_n]^T [m] [a]$$

$$\therefore \quad \ddot{D}_n + w_n^2 \times D_n = \frac{-f(t) \, . \, [\phi_n]^T [m] [a]}{R s_n} \qquad \text{..(32)}$$

$$\text{But } R_s = -\frac{[\phi_n]^T [m] [a]}{w_n^2}$$

$$\therefore \quad \ddot{D}_n + w_n^2 \, . \, Dn = w_n^2 \cdot f(t) \qquad \text{...(33)}$$

It can be shown (4) that the solution of Equation (33) with the initial condition of the dam being at rest, *i.e.*, for time $t=0$, $D_n=0$ and $\dot{D}_n=0$.

$$D_{n_T}=w_n\int_0^T f(t)\,.\,\sin w_n(T-t)\,.\,dt \qquad ...(34)$$

Where D_{n_T} is the value of the dynamic factor at time $t=T$.

Equation (34) is suitable only if $f(t)$ is an integrable function. As already pointed out the quake load would be random, so the equivalent expression for such condition is given by Equation (35)(3).

$$D_{n_T}=w_n\sum_0^T \Delta t\,.\,f(t)\,.\sin w_n(T-t) \qquad ...(35)$$

Equation (35) would now be solved for various mode shapes. It may, however, be noted from Table VI that R_{s_2}, R_{s_5} and R_{s_6} are equal to zero so the dynamic values R_2, R_5, and R_6 for these modes will be zero

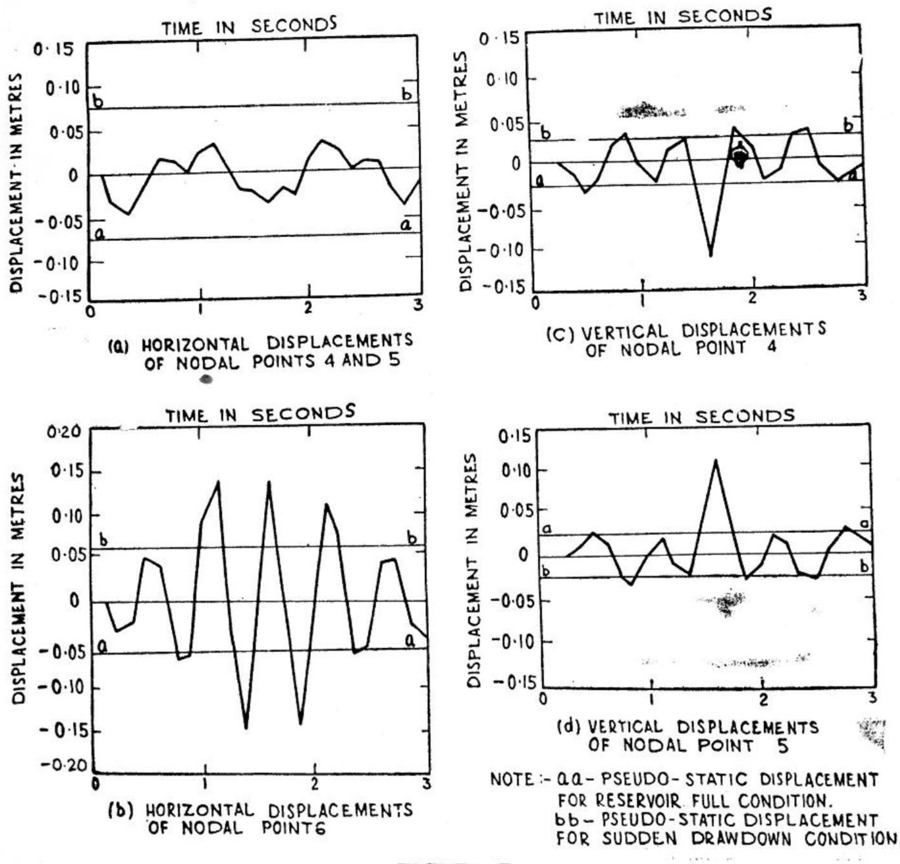

FIGURE 7.

irrespective of the values of the corresponding dynamic load factors. This means the horizontal quake load does not excite those symmetrical modes. Hence Equation (35) need be solved for the 1st, 3rd and the 4th modes. The computations are shown in Table VIII.

The interval $\triangle t$ is choosen as $\frac{1}{8}$ sec. This interval touches the values of $f(t)$ as 1, 0 and -1 in succession. For more accurate results

TABLE VIII

T	D_1	D_3	D_4	R_1	R_3	R_4
0	0·000	0·000	0·000	0·000	0·000	0·000
$\frac{1}{8}$	0·000	0·000	0·000	0·000	0·000	0·000
$\frac{1}{4}$	0·345	0·818	1·280	–0·250	0·055	0·100
$\frac{3}{8}$	0·568	0·907	0·632	–0·412	0·060	0·049
$\frac{1}{2}$	0·243	–0·628	–2·248	–0·176	–0·041	–0·175
$\frac{5}{8}$	–0·170	–1·604	–1·742	0·123	–0·106	–0·136
$\frac{3}{4}$	–0·176	–0·335	2·667	0·128	–0·022	0·208
$\frac{7}{8}$	–0·124	1·233	3·056	0·090	0·081	0·238
1	–0·365	0·886	–2·435	0·265	0·058	–0·190
$1\frac{1}{8}$	–0·476	–0·250	–4·259	0·345	–0·017	–0·332
$1\frac{1}{4}$	–0·078	–0·346	1·609	0·057	–0·023	0·126
$1\frac{3}{8}$	0·344	–0·134	5·054	–0·250	–0·008	0·394
$1\frac{1}{2}$	0·306	–0·620	–0·390	–0·222	–0·041	–0·030
$1\frac{5}{8}$	0·164	–0·554	–5·247	–0·119	–0·037	–0·409
$1\frac{3}{4}$	0·300	–0·822	–0·924	–0·218	–0·054	–0·072
$1\frac{7}{8}$	0·324	1·466	4·791	–0·235	0·097	0·374
2	–0·103	–0·124	2·012	0·075	–0·008	0·157
$2\frac{1}{8}$	–0·489	–1·480	–3·797	0·355	–0·098	–0·296
$2\frac{1}{4}$	–0·361	–0·813	–2·610	0·262	–0·054	–0·204
$2\frac{3}{8}$	–0·115	0·480	2·508	0·084	0·032	0·196
$2\frac{1}{2}$	–0·163	0·637	2·571	0·118	0·053	0·200
$2\frac{5}{8}$	–0·143	0·227	–1·238	0·104	0·015	–0·100
$2\frac{3}{4}$	0·263	0·323	–1·904	–0·191	0·021	–0·149
$2\frac{7}{8}$	0·568	0·131	0·297	–0·412	0·009	0·023
3	0·332	–0·885	0·761	–0·241	–0·058	0·059

Note : 'T' represents time elapsed in seconds.

TABLE IX

T	Nodal points					
	4		5		6	
	r_x	r_y	r_x	r_y	r_x	r_y
0	0·0000	0·0000	0·0000	0·0000	0·0000	0·0000
$\frac{1}{8}$	0·0000	0·0000	0·0000	0 0000	0·0000	0·0000
$\frac{1}{4}$	—0·0263	0·0029	—0·0263	—0 0029	—0·0400	0·0000
$\frac{3}{8}$	—0·0431	—0·0100	—0·0431	0·0100	—0·0304	0·0000
$\frac{1}{2}$	—0·0161	—0·0304	—0·0161	0·0304	0·0467	0·0000
$\frac{5}{8}$	0·0168	—0·0166	0·0168	0·0166	0·0385	0·0000
$\frac{3}{4}$	0·0146	0·0271	0·0146	—0·0271	—0·0709	0·0000
$\frac{7}{8}$	0.0058	0·0361	0·0058	—0·0361	0·0673	0·0000
1	0·0218	—0·0033	0·0218	0·0033	0·0917	0·0000
$1\frac{1}{8}$	0·0329	—0·0205	0·0329	0·0205	0·1344	0·0000
$1\frac{1}{4}$	0·0074	0·0144	0·0074	—0·0144	—0·0455	0·0000
$1\frac{3}{8}$	—0.0217	0·0301	—0·0217	—0·0301	—0·1550	0·0000
$1\frac{1}{2}$	—0·0197	—0·0253	—0·0197	0·0253	—0.0078	0·0000
$1\frac{5}{8}$	—0·0339	—0·1049	—0·0339	0·1049	0·1339	0·0000
$1\frac{3}{4}$	—0·0189	—0·0224	—0·0189	0·0224	0·0054	0·0000
$1\frac{7}{8}$	—0·0261	0·0372	—0·0261	—0·0372	—0·1448	0·0000
2	0·0085	0·0201	0·0085	—0·0201	—0·0534	0·0000
$2\frac{1}{8}$	0·0347	—0·0206	0·0347	0·0206	0·1094	0·0000
$2\frac{1}{4}$	0·0274	—0·0134	0·0274	0·0134	0·0785	0·0000
$2\frac{3}{8}$	0·0066	0·0277	0·0066	—0·0277	—0·0604	0·0000
$2\frac{1}{2}$	0·0096	0·0313	0·0096	—0·0313	—0·0568	0·0000
$2\frac{5}{8}$	0·0085	—0·0049	0·0085	0·0049	0·0435	0·0000
$2\frac{3}{4}$	—0·0204	—0·0238	—0·0204	0·0238	0·0462	0·0000
$2\frac{7}{8}$	—0·0406	—0·0168	—0·0406	0·0168	—0·0288	0·0000
3	—0·0202	—0·0096	—0·0202	0·0096	—0·0432	0·0000

Note : All the displacements are in metres.

the interval $\triangle t$ should be much smaller so as to include the intermediate character of the function $f(t)$. As the demonstration of the concepts is the main aim of the present article the laborious calculations involving smaller values of $\triangle t$ have not been undertaken. For the same reason the calculations have been made for the first three seconds only. Actually the calculations should be made for the entire period during which the quake shock is felt.

Dynamic Displacements

With the help of the values of '*R*' in Table VIII and the normalised mode shapes given in Table V, the dynamic displacements are calculated as shown in Table IX. Figure 7 shows the comparison between the pseudo-static and dynamic displacements.

Dynamic Stresses

The dynamic stresses may be calculated with the help of the dynamic displacements (Table IX) by following the method demonstrated in reference (1). Due to small number of nodal points the stress calculations would not serve any practical purpose, hence the stress calculations are omitted in the present article.

Conclusion and Remarks

The dynamic horizontal displacements of nodal points 4 and 5 are lower whereas that of the nodal point 6 are higher than their pseudo-static counterparts. It is thus likely that in the upper regions of the dam the pseudo-static approach may be inadequate whereas for the lower regions of the dam the same approach may be conservative in predicting the displacements under the dynamic loads.

For the dynamic analysis to be of practical interest (*a*) large number of small size elements should be considered and (*b*) time interval $\triangle t$ should be very small. Such an analysis would obviously need one of the most laborious computer programmings.

References

(1) Parikh, S.K. : "Analysis of Earthen Dams by the Method of Finite Elements". Journal of Indian National Society of Soil Mechanics and Foundation Engineering, Vol. 9, No. 2, April 1970.

(2) Parikh, S.K. : "Aseismic Design of Earthen Dams". Golden Jubilee Number of Institute of Engineers, Poona-Centre, January 1970.

(3) Hurty, W.C. and Rubinstein, H.F. : "Dynamics of Structures". Prantice Hall, Inc., 1964.

(4) Norris and others : "Structural Design for Dynamic Loads". McGraw Hill Book Co., Inc., 1959.

(5) Clough, R.W. and Chopra, A.K. : "Earthquake Analysis in Earthen Dams". Vol. 92, No. EM 2, April 1966, Journal of Engineering Mechanics Division. Proc. A.S.C.E., Paper No. 4793, pp. 197-211.